MicroRNA-137-mediated inhibition of lysine-specific demethylase-1 prevents against rheumatoid arthritis in an association with the REST/mTOR axis

Wei Sun[1], Yijun Zhang[1], and Guanghui Wang[2] (iD)

Abstract

Background: It has been increasingly reported that microRNAs (miRNAs) are related to rheumatoid arthritis (RA) pathogenesis. This present research was conducted to analyze the functions of miR-137 and the underlying molecular mechanism in RA progression.

Methods: Differentially expressed miRNAs in RA patients were analyzed using microarray-based analyses. Next, experiments involving miR-137 overexpression were performed to analyze the role of miR-137 in human fibroblast-like synoviocytes-RA (HFLS-RA) using cell counting kit-8 (CCK-8) assay, EdU staining, Transwell assay and flow cytometry, respectively. The function of miR-137 in inflammation was determined using ELISA. The binding relationship between miR-137 and LSD1 was confirmed by dual-luciferase reporter gene assay and ChIP test. Besides, a rat model with RA was established for *in vivo* experiments.

Results: miR-137 was downregulated in RA tissues and cells, which was negatively correlated with inflammatory factors. Upregulated miR-137 suppressed growth, migration and invasion of HFLS-RA, but promoted apoptosis. Lysine-specific demethylase-1 (LSD1) was a target of miR-137 and could be negatively regulated by miR-137. Moreover, LSD1 could activate REST through demethylation, while the REST/mTOR pathway induced levels of pro-inflammatory factors in RA. We observed the similar results in our *in vivo* study.

Conclusion: This study suggested that miR-137 reduced LSD1 expression to inhibit the activation of REST/mTOR pathway, thus preventing against inflammation and ameliorating RA development. Our research may offer new insights into treatment of RA.

Introduction

Rheumatoid arthritis (RA) is a frequent chronic symmetrical autoimmune disease, which affects diarthrodial joints activities.[1] RA, as a multifactorial disease, often contributes to articular damage, loss of mobility and even reduction in life expectancy due to the chronic inflammation of synovial joints.[2] Normally, synovial fibroblasts are mainly responsible for synovial homeostasis.[3] However, the RA human fibroblast-like synoviocytes (HFLS-RA) are likely to induce cartilage erosion and trigger inflammation as well as autoimmunity.[4,5]

[1]Department of Sports Medicine, Qilu Hospital (Qingdao), Cheeloo College of Medicine, Shandong University, Shandong, P.R. China
[2]Department of Orthopaedics Oncology, Qilu Hospital (Qingdao), Cheeloo College of Medicine, Shandong University, Shandong, P.R. China

Corresponding Author:
Guanghui Wang, Department of Orthopaedics oncology, Qilu Hospital (Qingdao), Cheeloo College of Medicine, Shandong University, No. 758, Hefei Road, Shibei District, Qingdao 266035, Shandong, P.R. China.
Email: ghwang4056@163.com

Therefore, to get a better understanding on the mechanism affecting HFLS-RA function is of clinical value in terms of RA therapy. Dysregulated microRNAs (miRNAs) have been the focus of recent studies in HFLS-RA, which may contribute to RA pathogenesis or act as diagnostic biomarkers.[6–8]

miRNAs are small non-coding RNA molecules, which serve as key regulators of mRNA translation or mRNA stability to negatively regulate gene expression.[9] Among them, miR-137 is located on chromosome 1p22 and has been revealed as a regulator of susceptibility genes in RA by mediating the function of HFLS-RA.[10] Moreover, miR-137 was poorly expressed in cartilage tissues of rats and patients with osteoarthritis, and upregulation of miR-137 could inhibit inflammatory factor levels and extracellular matrix degradation.[11,12] Nevertheless, the detailed molecular mechanism underlying miR-137 in RA awaits to be further investigated. It was demonstrated that miR-137 targets lysine-specific demethylase-1 (LSD1) during neurodevelopment.[13] LSD1 (also termed as KDM1A), is an enzyme dependent on flavin adenine dinucleotide, which regulates expression of genes through H3K4me1/2 or H3K9me1/2.[14,15] Besides, it has been found previously that knockdown of LSD1 could ameliorate RA at the early stage by repressing $CD4^+$ T cell proliferation and the production of cytokines, including IFN-γ, IL-17 and IL-10.[16] Also, LSD1 can modulate endochondral ossification during fracture healing, which will benefit the understanding of bone regeneration.[17] In addition, LSD1 is reported to mediate repressor element-1 silencing transcription factor (REST) expression in small cell lung carcinoma at the transcriptional level,[18] while REST is also involved in the RA-induced peripheral neuropathy.[19] Besides, downregulation of the protein kinase B (Akt)/mammalian target of rapamycin (mTOR) is correlated with the inhibited proliferation, migration and invasion of HFLS-RA and reduced proinflammatory factors.[20,21] However, how REST affected mTOR in RA is rarely known. Thus, we aim to testify our assumption that miR-137/LSD1/REST/mTOR participates in RA progression, and meanwhile, to investigate the influence of the potential mechanism on HFLS-RA by examining the effects of miR-137/LSD1/REST/mTOR on HFLS-RA, with the ultimate goal of providing novel insights for RA therapy.

Materials and methods

Ethical statement

The protocol for this study was approved by the Ethics Committee of Qilu Hospital (approval number: MECSDUMS 2015035), and all participators provided their written informed consent prior to the enrollment.

All experiments involving animals were approved and conducted according to the *Guide for the care and use of laboratory animals*, and the experimental procedures were authorized by the Animal Ethics Committee of Qilu Hospital (approval number: 2017002).

Study objects

A total of 63 RA patients who met the 2010 classification criteria of American College of Rheumatology or European League against Rheumatism and hospitalized in Qilu Hospital from January 2016 to January 2017 were included in this study. The value of Disease Activity Score including a 28-joint count (DAS28) was higher than 3.2 among these patients. All patients did not receive any immunotherapy or disease modifying antirheumatic drug triple therapy before recruitment. Pregnant women or patients during the lactation period were excluded. All the clinical data and DAS28 scores were assessed in the course of treatment and follow-up. Synovial tissue samples obtained from healthy people in Qilu Hospital were taken as control. Details of RA patients and controls are shown in Table 1.

Tissue collection and RNA extraction

Blood from the patients was collected in an ethylene diamine tetraacetic acid (EDTA)-coated bottle and stored at $-80°C$, while total RNA was extracted by chloroform-isopropanol extraction. Specifically, the samples were subjected to vortex at room temperature for 15 min followed by centrifugation at $10,000 \times g$ and $4°C$ for 10 min. The supernatant was then mixed with $200 \mu L$ chloroform for 15 min and centrifuged at $12,000 \times g$ and $4°C$ for 15 min. The supernatant was mixed with $500 \mu L$ isopropanol for 10 min, and the mixture was centrifuged at $12,000 \times g$ and $4°C$ for 10 min. Being washed twice with 75% ethanol (1 mL), the mixture was centrifuged again at $7,500 \times g$ for 5 min. The precipitate was dissolved again in 30 mL RNAse-free water. The purity and concentration of the total RNA

Table 1. Demographic characteristics of study objects.

Variables	Control (n = 63)	RA (n = 63)
Age (mean $\pm$ SD)	48.48 ± 8.12	45.17 ± 7.14
Sex (Male/Female)	9/54	12/51
DAS28		
<3.2	0	63
3.2–5.1	48	0
>5.1	15	0

RA, rheumatoid arthritis; DAS28, Disease Activity Score including a 28-joint count; SD, standard deviation.

were determined using a dual-beam ultraviolet spectro-photometer (Eppendorf, Germany).

Microarray-based analysis

Serum and synovial tissues from three patients and controls were selected, whilst total RNA molecules were extracted using TRIzol Reagent (Thermo Fisher Scientific, Waltham, MA, USA), which were synthesized into complementary DNA (cDNA) using a TaqMan miRNA Reverse Transcription kit (Thermo Fisher Scientific). Next, miRNA molecules were labeled with miRNA Complete Labeling and Hyb Kit (Agilent Technologies, Santa Clara, CA, USA), while hybridization was implemented using Human miRNA Microarray (Agilent), followed by scanning with Agilent SureScan Dx (Agilent). Raw data were corrected and normalized by RMA algorithm. Differentially expressed miRNAs were selected at the threshold of $p < 0.01$ and FoldChange < -2, which were plotted as a heatmap.

Reverse transcription quantitative polymerase chain reaction (RT-qPCR)

Extracted RNA was synthesized into cDNA by a TaqMan miRNA Reverse Transcription kit (Thermo Fisher Scientific), followed by PCR reaction using a QuantiFast SYBR Green RT PCR kit (Qiagen, Hilden, Germany) on an ABI7900 real-time PCR system (Thermo Fisher Scientific). The primers for miR-137, LSD1, REST and internal references U6 and glyceraldehyde-3-phosphate dehydrogenase (GAPDH) in this experiment are shown in Table 2. Specifically, miR-137 was normalized to U6, whereas LSD1 and REST were normalized with GAPDH. The relative expression of genes was evaluated by $2^{-\triangle\triangle CT}$ method.

HFLS-RA cell treatment

HFLS-RA (inflammatory cells) and human fibroblast-like synoviocytes (HFLS, control cells) were commercially obtained (Jennio Biotechnology Co., Ltd., Guangzhou, Guangdong, China) and cultured in high-glucose Dulbecco's modified Eagle's medium (DMEM; Thermo Fisher Scientific) or minimal essential medium (MEM; Thermo Fisher Scientific), respectively. Overexpression vectors for miR-137, LSD1 and REST were synthesized by GenePharma (Shanghai, China).

Prior to cell transfection, the cells were seeded in 6-well plates with 5×10^5 cells/well. Next, the cells were transfected with overexpression plasmids using Lipofectamine 3000 (Invitrogen, Carlsbad, CA, USA). Specifically, a total of 100 pmoL overexpression plasmids or 5 μL liposomes was mixed with 125 μL Opti-MEM (Invitrogen), respectively, which was incubated at room temperature under serum-free conditions for 10 min to form the transfection complex. The culture medium was renewed with DMEM (American Type Culture Collection, Manassas, VA, USA) after 6 h of incubation at 37°C in 5% CO_2 for further experiments. REST-transfected cells were further co-cultured with 5 mM mTOR pathway inhibitor-3 (HY-18353, MedChemExpress, Monmouth Junction, NJ, USA) for 48 h for subsequent experiments.

Cell counting kit-8 (CCK-8) assay

The transfected cells were seeded into 96-well plates with 1×10^4 cells/well, followed by evaluation using a CCK-8 kit (Promega, Madison, WI, USA) on day 1, 2, and 3 post-transfection, respectively. Briefly, the previous medium was renewed by 100 μL fresh medium and 10 μL CCK-8 reagent, which was incubated at 37°C for 4 h. Then, the optical density (OD) value at 490 nm was measured by a microplate reader (Bio-Rad, Hercules, CA, USA).

Table 2. Primers for RT-qPCR.

Targets	Primer sequences (5′-3′)
miR-137	F: 5′-GCGCTTATTGCTTAAGAATAC-3′
	R: 5′-CAGTGCAGGGTCCGAGGT-3′
LSD1	F: 5′ AGTTCAGAATTCATGGAGCAGAAACTC3′
	R: 5′-TCAACATCTAGATCACATGCTTGGGGACTGC-3′
REST	F: 5′-CGCCCATATAAATGTGAACTTTGTC-3′
	R: 5′-GGCGGGTTACTTCATGTTGATTAG-3′
U6	F: 5′-GCTTCG GCAGCACATATACTAAAAT-3′
	R: 5′-CGCTTC ACGAATTTGCGTGTCAT-3′
GAPDH	F: 5′-TGGAATCCACTGGCGTCTTC-3′
	R: 5′ GGT TCACGCCCATCACAAAC-3′

RT-qPCR, reverse transcription quantitative polymerase chain reaction; miR-137, microRNA-137; LSD1, Lysine-specific demethylase-1; REST, repressor element-1 silencing transcription factor; GAPDH, glyceraldehyde-3-phosphate dehydrogenase; F, forward; R, reverse.

5-Ethynyl-2'-deoxyuridine (EdU) assay

The stably-transfected cells were seeded in 96-well plates with 1×10^4 cells/well. After 48 h-transfection, cell proliferation was analyzed by a Cell-Light EdU Apollo567 In Vitro kit (RiboBio, Guangzhou, Guangdong, China). Specifically, the cells in each well were reacted with $100 \, \mu L$ fresh medium containing $50 \, \mu M$ EdU at $37°C$ for 18 h. Following that, the cells in each well were fixed with $100 \, \mu L$ 4% formaldehyde for 30 min at room temperature, and incubated with 0.5% Triton X-100 for 10 min at room temperature. After the incubation with $100 \, \mu L$ $1 \times$ Apollo reaction cocktail for 30 min, the nuclei were stained with $100 \, \mu L$ 4′,6-diamidino-2-phenylindole (DAPI; Solarbio, Beijing, China) for 30 min. Five fields of view were randomly selected for evaluation under a fluorescence microscope (BX43, Olympus).

Transwell assay

In the Transwell invasion assay, HFLS-RA and HFLS (2×10^4) were suspended in serum-free DMEM and seeded in the Transwell apical chamber (BD Biosciences, San Jose, CA, USA) pre-coated with Matrigel (BD Biosciences). Meanwhile, Transwell basolateral chamber was added with DMEM containing 20% fetal bovine serum (FBS). After 48 h of cell culture, the cells on the membrane surface were wiped with cotton swabs, fixed with methanol for 30 min at room temperature, and stained with 0.1% crystal violet (Sigma-Aldrich, St Louis, MO, USA). The cells were imaged by an inverted optical microscope (IX71, Olympus) with five visual fields randomly selected for cell counting. During Transwell migration assay, procedures were similar except for the usage of pre-coated Matrigel.

Flow cytometry

HFLS-RA and HFLS were seeded in 6-well plates (5×10^5 cells/well) for cell cycle analysis. Briefly, the cells were cultured with $50 \, mg/L$ propidium iodide (PI) containing 1 mL RNase and $5 \, \mu L$ 7-aminoactinomycin D (BD Biosciences) for 30 min in the dark. Cell cycle at 488 nm wavelength was analyzed using a Coulter Epics XL flow cytometer (Beckman Coulter, Fullerton, CA, USA) after filtration with 100-mesh nylon mesh.

Apoptosis was analyzed by Annexin V-fluorescein isothiocyanate (FITC)/PI double staining. The cells were resuspended using $200 \, \mu L$ binding buffer (BD Biosciences). Subsequently, the cell suspension was fully mixed with $10 \, \mu L$ protein Annexin V-FITC and $5 \, \mu L$ protein PI for 15 min in void of light, followed by the addition of $300 \, \mu L$ protein binding buffer. Apoptosis at 488 nm wavelength was also analyzed by Coulter Epics XL flow cytometer (Beckman Coulter, Chaska, MN, USA).

Enzyme-linked immunosorbent assay (ELISA)

Expression of inflammatory factors interleukin (IL)-1β, IL-6 and cyclooxygenase-2 (COX2) was determined by ELISA. The transfected HFLS-RA were seeded in 24-well plates (2×10^5 cells/well) and cultured in DMEM containing 10% FBS for 48 h at $37°C$. The supernatant was collected by centrifugation at $1,000 \times g$ for 5 min at $4°C$. Release of IL-1β, IL-6 and COX2 in cells was assessed using human IL-1β ELISA kit, human IL-6 ELISA kit (R&D Systems, MA, USA), or human COX2 ELISA kit (Abcam, Cambridge, UK), respectively. The concentration of inflammatory factors was determined by ELISA spectrophotometer (Molecular Devices, San Jose, CA, USA).

Dual-luciferase reporter gene assay

Binding sites between miR-137 and LSD1 were predicted by StarBase (http://starbase.sysu.edu.cn), TargetScan (http://www.targetscan.org), RNA22 (https://cm.jefferson.edu/rna22), miRanda (https://omictools.com/miranda-tool), PITA (www.pita.org), and miRDB (www.mirdb.org). The sequence containing the binding site of wild type (Wt) or mutant type (Mut) of miR-137 was synthesized by GenePharma (Shanghai, China), which was inserted into pGL3 control vectors (Thermo Fisher Scientific). For luciferase reporter gene detection, HFLS-RA were seeded into 24-well plates for 24 h and co-transfected with 100 ng Wt-LSD1/Mut-LSD1 plasmids and 100 nM miR-137 mimic using Lipofectamine 2000. Luciferase activity was measured by a dual-luciferase reporter gene 1000 detection system (Promega) with normalization to Renilla luciferase.

Western blot analysis

A total of 2×10^6 HFLS-RA were lysed using radio immunoprecipitation assay buffer (Beyotime Biotechnology, Shanghai, China) at $4°C$, and centrifuged at $1,000 \times g$ for 5 min to collect the supernatant. The protein concentration was determined with a bicinchoninic acid protein assay kit (Beyotime Biotechnology). A total of 30 g protein was separated by 10% sodium dodecyl sulfate (SDS)-polyacrylamide gel electrophoresis and transferred to a polyvinylidene fluoride membrane (Bio-Rad), which was incubated with 5% skimmed milk for 1 h at room temperature. The membrane was probed overnight with primary

rabbit monoclonal antibodies to LSD1 (1:20000, ab129195, Abcam), mTOR (1:1000, ab32028, Abcam), p-mTOR (1:5000, ab109268, Abcam), and GAPDH (1:3000, 875174, Cell Signaling Technologies, Beverly, MA, USA) at 4°C. Following that, the membrane was incubated with horseradish peroxidase-labeled goat anti-rabbit secondary antibody (1:10000, ab205718, Abcam). Protein bands were detected using an Enhanced Chemiluminescence-Plus kit (Thermo Fisher Scientific) with GAPDH used as internal reference.

Chromatin immunoprecipitation (ChIP)

The HFLS-RA were incubated with 1% formaldehyde for 10 min, followed by further incubation with 0.125 M glycine for 10 min. After the addition of SDS lysis buffer and protease inhibitor complex (Thermo Fisher Scientific), the cells were disrupted by ultrasonication, centrifuged to remove insoluble impurities, and mixed with 900 µL ChIP dilution buffer (Thermo Fisher Scientific), 20 µL 50 × protease inhibitor cocktail, as well as 60 µL ProteinA Agarose at 4°C for 1 h. The cells were then centrifuged at $1,000 \times g$ for 1 min to harvest the supernatant, which was then incubated with IgG antibody (1:3000, ab172730, Abcam) and miR-137 antibody (Santa Cruz Biotechnology, Santa Cruz, CA, USA) overnight at 4°C. Each tube was incubated with 250 µL buffer to flush the precipitation complex for 15 min at room temperature. Crosslinking was reversed with 20 µL 5 M NaCl, whereas the recycled DNA fragments were dissolved in 100 µL ddH_2O for PCR analysis.

Establishment of RA rat model

Forty male Wistar rats (aged 7–8 weeks old; weighing 105 ± 15 g) were purchased from Charles River Laboratories (Beijing, China) and housed at constant temperature of 25°C. The rats were allowed to have free access to food and water in a 12-h light-dark cycle. Another 30 rats in the RA group were subjected to collagen type II-induced arthritis (CIA). Specifically, collagen type II (Southern Biotech, Birmingham, AL, USA) was dissolved in 0.05 M acetic acid to a final concentration of 2 mg/mL, which was vortexed overnight at 4°C. Subsequently, the solution was then emulsified with Freund's incomplete adjuvant (Sigma-Aldrich) at a ratio of 1:1 to a final concentration of 1 mg/mL. The rats were subcutaneously injected with the emulsion into their tails on day 1 (300 µL) and day 8 (200 µL).[22] Control rats were treated with saline.

Arthritic scoring

Arthritic scoring was conducted on each hind paw of rats induced by CIA on a scale of 0–4 with the average score recorded. Specifically, the rats without swelling or redness scored 0; slight swelling or redness, 1; gradual swelling or redness from the ankle to the midfoot, 2; swelling and inflammation of the entire limb, 3; swelling and inflammation of the entire lamb with a loss of mobility, 4. The total score for rats was 16 (with score of 4 each limb) during the arthritic scoring. The successful modeling was manifested by arthritic score >6.[23]

Pain score in rats

Experimental animals were scored for pain based on the Method for the Assessment of Pain Levels in Laboratory Animals (http://www.ndmctsgh.edu.tw/animal/), which focuses on the body weight, appearance, clinical signs, innate behavior and response to stimuli. The pain assessment items were scored as 1 if they met the mild level, 2 if they met the moderate level, 3 if they met the severe level, and 0 if they did not meet any of the assessment items. The cumulative score for each assessment item was performed for each experimental rat, and then the total score was statistically analyzed.

Hematoxylin-eosin (HE) staining

Histopathological analysis of the paw joint was performed. After removing the skin, superficial muscles and tissues, the paw joints were excised from the right hind limb of the rats and then fixed in 4% polyformaldehyde solution at 4°C for 1 week. Fixed samples were decalcified in 14% EDTA solution at 4°C for 35 days to make the joints soft. The joints were dehydrated with gradient alcohol, embedded in paraffin and sectioned into 4–6 µm thickness, which were placed in poly-L-lysine-coated slides.[23] The sections were then dewaxed in xylene and rehydrated by decreasing concentrations of ethanol. A HE Staining Kit (Solarbio, Beijing, China) was then utilized to observe the histological changes of synovial tissues. In brief, tissues were stained in hematoxylin for 15 min and then differentiated in 1% hydrochloric acid alcohol for 30 s. After another 5-min eosin staining, the sections were dehydrated, sealed and observed under a microscope (IX71, Olympus) with five visual fields randomly selected for photographing.

Statistical analysis

We analyzed statistical data using GraphPad Prism version 7.00 (GraphPad Software, San Diego, CA, USA). Data from at least three independent experiments were

presented as mean ± SD. Intragroup comparisons were made using unpaired *t*-test or one-way analysis of variance (ANOVA) and Tukey's post hoc test. When *p* value <0.05, data were statistically significant.

Results

Poor expression of miR-137 is detected in HFLS-RA

Microarray-based analyses were conducted on the collected sera and synovial tissues of three randomly selected RA patients or healthy controls. miR-137 was downregulated in RA-related microarray (Figure 1(a) and (b)). The expression of miR-137 in serum and synovial tissues of RA patients was further confirmed by RT-qPCR, which showed the same results as those of microarray-based analyses (Figure 1(c) and (d)). Besides, pro-inflammatory factors IL-1β, IL-6, and COX2 levels in sera of RA patients and healthy control were detected by ELISA. The levels of inflammatory factors were found to be increased in RA patients (Figure 1(e)). Moreover, the correlation analysis of miR-137 expression with the levels of pro-inflammatory factors revealed that miR-137 expression was negatively correlated with levels of IL-1β, IL-6 and COX2 (Figure 1(f)). Results of RT-qPCR further validated that miR-137 expression in HFLS-RA was lower than that in HFLS (Figure 1(g)).

Upregulation of miR-137 suppresses growth of HFLS-RA

In order to determine the role miR-137 played in HFLS-RA, miR-137 was upregulated in HFLS-RA by transfection of miR-137 mimic. RT-qPCR was
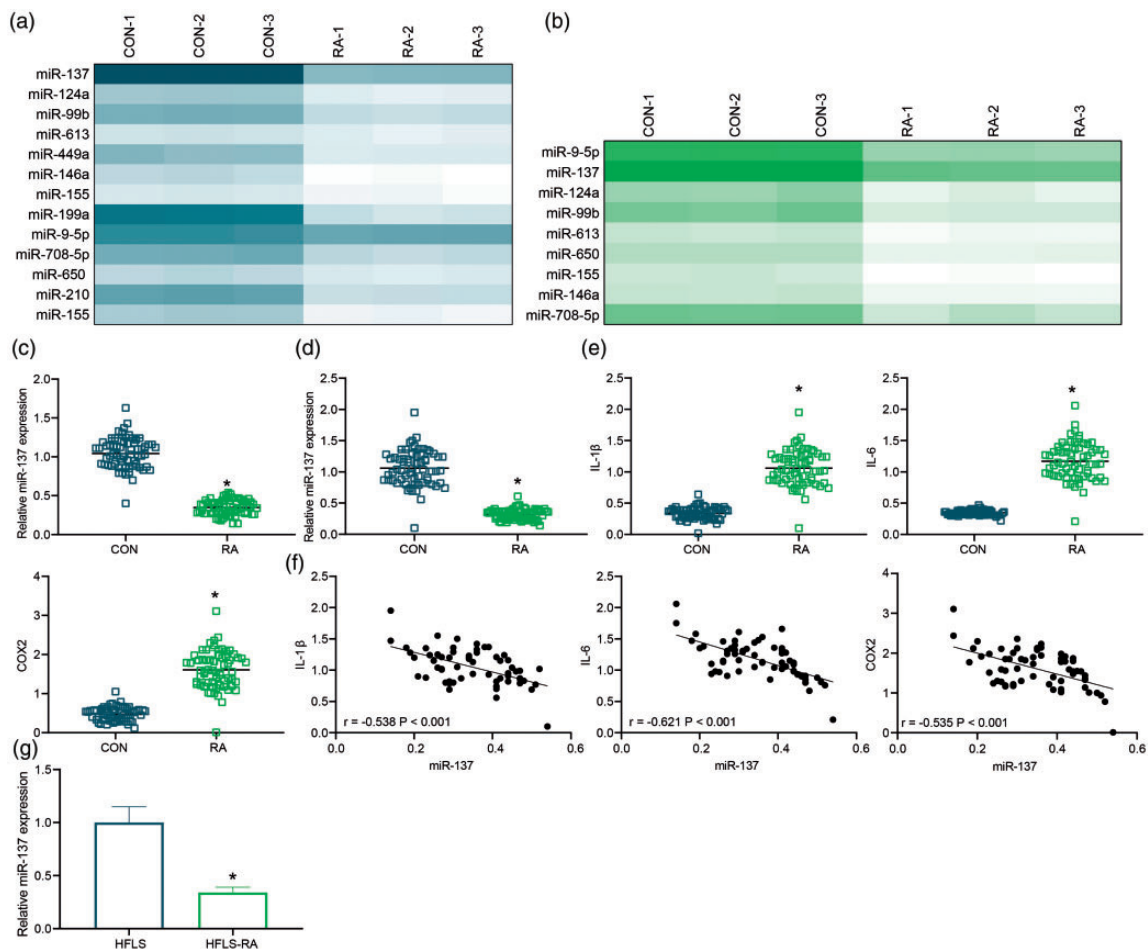

Figure 1. Decreased expression of miR-137 is detected in RA. (a and b), Differentially expressed miRNAs in sera and synovial tissues of RA patients or healthy control determined by microarray-based analyses (the data in the heatmap are sorted by the FC values). (c and d) Expression of miR-137 in sera and synovial tissues of RA patients or healthy control detected using RT-qPCR. (*p < 0.05; analyzed using two-way ANOVA). (e) Levels of IL-1β, IL-6 and COX2 in serum of RA patients or healthy control examined using ELISA (*p < 0.05; analyzed using two-way ANOVA). (f) Correlation of miR-137 expression with pro-inflammatory factor levels. (g) Expression of miR-137 in HFLS-RA or HFLS determined by RT-qPCR (*p < 0.05; analyzed using unpaired *t*-test). All samples were prepared in triplicate and all measures were performed three times. miR, microRNA; RA, rheumatoid arthritis; FC, foldchange; RT-qPCR, reverse transcription quantitative polymerase chain reaction; ANOVA, analysis of variance; IL, interleukin; COX2, cyclooxygenase-2; HFLS, human fibroblast-like synoviocytes.
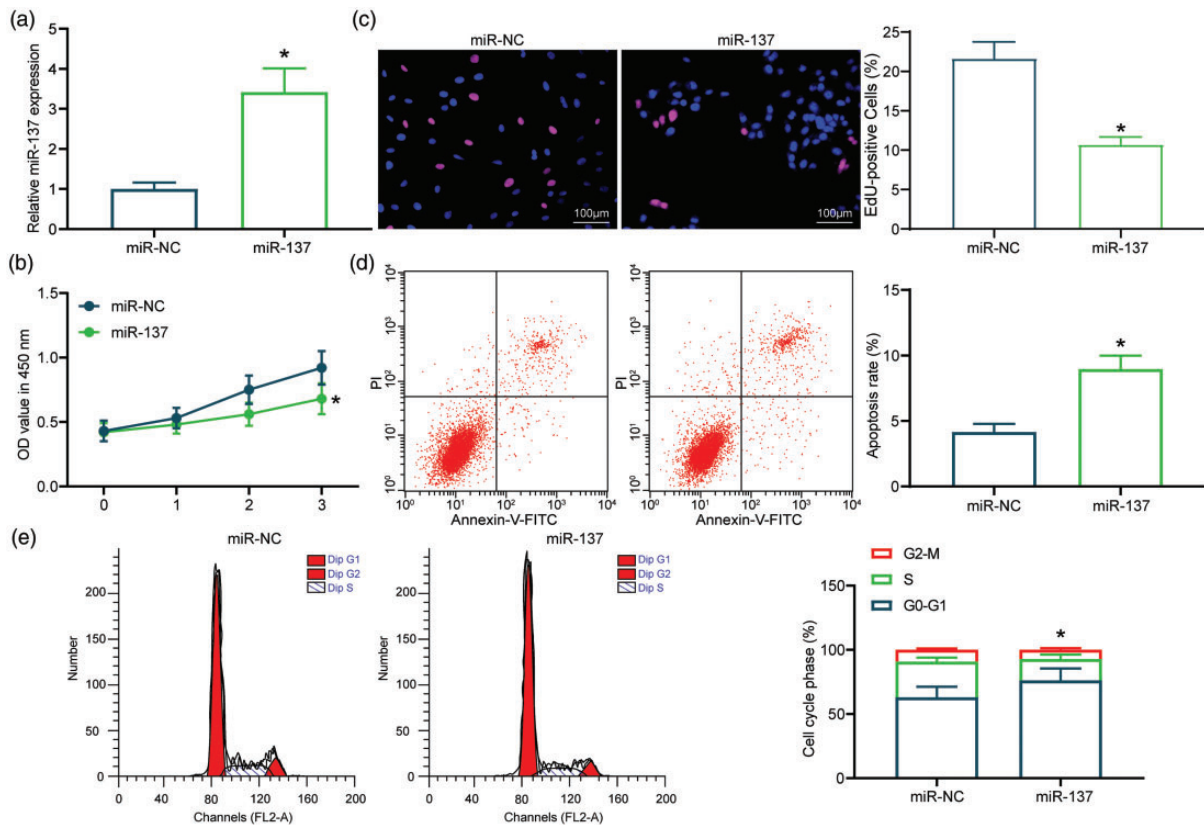
Figure 2. miR-137 suppresses growth of HFLS-RA but promotes the cell apoptosis. (a) Transfection efficiency of miR-137 overexpression plasmid detected by RT-qPCR (*$p < 0.05$; analyzed using unpaired t-test). (b) Growth of HFLS-RA examined by CCK-8 assay (*$p < 0.05$; analyzed using two-way ANOVA). (c) HFLS-RA viability determined using EdU assay with color red indicated EdU positive-cells while color blue represented DAPI positive-cells (*$p < 0.05$; analyzed using unpaired t-test). (d) Apoptosis of HFLS-RA assessed by flow cytometry. The apoptotic cells were shown in the top right corner (*$p < 0.05$; analyzed using unpaired t-test). (e) Cycle of HFLS-RA evaluated by flow cytometry (*$p < 0.05$; analyzed using two-way ANOVA). All samples were prepared in triplicate and all measures were performed three times. miR, microRNA; RA, rheumatoid arthritis; RT-qPCR, reverse transcription quantitative polymerase chain reaction; ANOVA, analysis of variance; HFLS, human fibroblast-like synoviocytes; CCK-8, cell counting kit-8; EdU, 5-Ethynyl-2′-deoxyuridine; DAPI, 4′,6-diamidino-2-phenylindole.

performed to detect the transfection efficiency, which showed that miR-137 was indeed upregulated (Figure 2 (a)). CCK-8 assay was then carried out to detect the growth of cells overexpressing miR-137. miR-137 mimic curtailed the growth of HFLS-RA (Figure 2(b)). Similarly, EdU results found that miR-137 overexpression reduced the DNA replication activity of cells (Figure 2(c)). Meanwhile, as results of flow cytometry shown, overexpressed miR-137 induced cell apoptosis and arrested more HFLS-RA at the G0/G1 phase, but less HFLS-RA at the S phase (Figure 2(d) and (e)). Results suggested that miR-137 suppressed the growth of HFLS-RA, promoted cell apoptosis, and decreased cell viability.

Migration, invasion and inflammatory response of HFLS-RA are suppressed by miR-137

Migratory and invasive capabilities of HFLS-RA were evaluated by Transwell assay. After 24 h incubation in the Transwell chamber, the number of cells migrated to the Transwell basolateral chamber was observed under the microscope, which showed that there were less cells transfected with miR-137 mimic migrated to the basolateral chamber (Figure 3(a)). Meanwhile, the invasion ability of cells transfected with miR-137 mimic to the basolateral chamber through Matrigel was weaker (Figure 3(b)). Since inflammatory factors play a role in RA pathogenesis, inflammatory factors IL-1β, IL-6 and COX2 levels were measured by ELISA, the results of which showed that overexpression of miR-137 decreased levels of IL-1β, IL-6 and COX2 (Figure 3(c)). Collectively, miR-137 could alleviate inflammatory response, migration, and invasion of HFLS-RA.

LSD1 is a target gene of miR-137

Next, mechanistic investigation was conducted. The target genes of miR-137 were predicted using starBase,
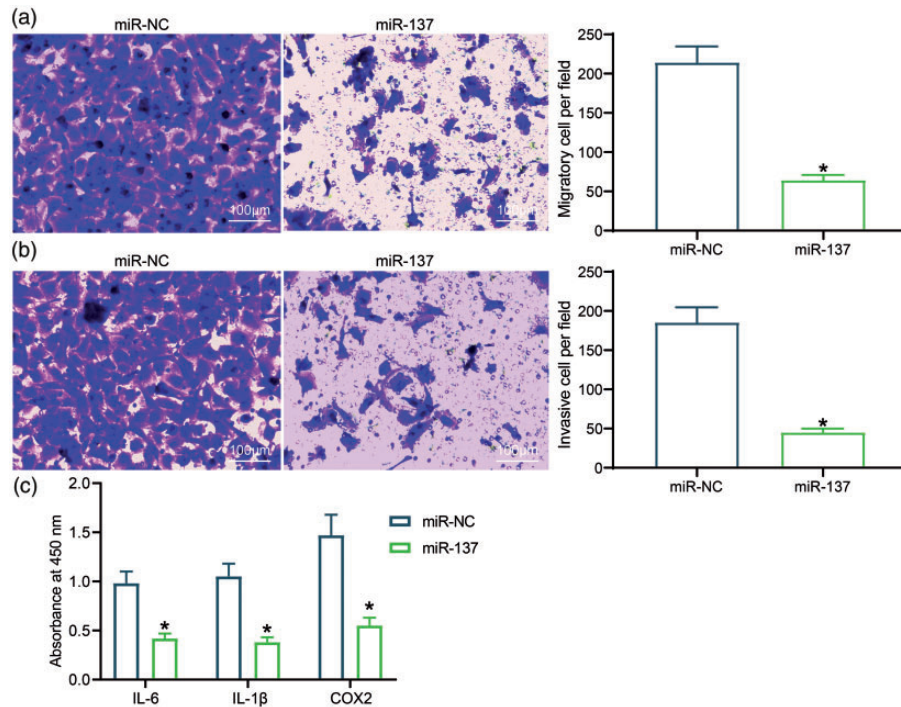
Figure 3. miR-137 inhibits invasion, migration and inflammation of HFLS-RA. (a and b) Migratory and invasive ability of HFLS-RA evaluated by Transwell assay (*$p < 0.05$; analyzed using unpaired *t*-test). C, Levels of inflammatory factors IL-1β, IL-6 and COX2 detected by ELISA (*$p < 0.05$; analyzed using two-way ANOVA). All samples were prepared in triplicate and all measures were performed three times. miR, microRNA; RA, rheumatoid arthritis; ANOVA, analysis of variance; IL, interleukin; COX2, cyclooxygenase-2; HFLS, human fibroblast-like synoviocytes; ELISA, enzyme-linked immunosorbent assay.

TargetScan, RNA22, miRanda, PITA and miRDB, the results of which were then intersected. KDM1A, which was also known as LSD1, was emerged (Figure 4(a)). The expression of LSD1 in RA patients and healthy control was further determined using RT-qPCR, which showed that LSD1 expression was elevated in sera and synovial tissues of RA patients (Figure 4(b)). It was revealed that miR-137 was negatively correlated with LSD1 expression in sera and synovial tissues (Figure 4 (c)). Moreover, results of dual-luciferase reporter gene assay unraveled that miR-137 could bind to LSD1 in HFLS-RA (Figure 4(d)). Further RT-qPCR and Western blot analysis showed that LSD1 expression was elevated in HFLS-RA, which could be downregulated by overexpression of miR-137 (Figure 4(e) and (f)). Besides, transfection of LSD1 overexpression plasmid significantly increased LSD1 expression (Figure 4(g) and (h)), but lowered the protein expression of pro-inflammatory factors (Figure 4(i)).

LSD1 reverses the effects of miR-137 on HFLS-RA

To explore the role of miR-137/LSD1 in RA, miR-137 and LSD1 were both overexpressed in HFLS-RA, followed by detection of transfection efficiency using RT-qPCR (Figure 5(a)). After the cells overexpressing

both miR-137 and LSD1 were successfully established, results of EdU assay showed that the number of positive cells was increased (Figure 5(b)), while flow cytometry displayed that the number of PI-Annexin V-positive cells decreased (Figure 5(c)), that is, LSD1 reversed the effect of miR-137 to increase cell viability. Furthermore, ELISA displayed that the levels of IL-1β, IL-6 and COX2 were all elevated after overexpression of miR-137 and LSD1 (Figure 5(d)). Therefore, compared to the decrease in cell activity by miR-137 mimic in Figure 2, LSD1 reversed the effect of miR-137 to significantly increase cell activity, indicating that LSD1 was a downstream factor of miR-137.

REST is a downstream effector of LSD1

The downstream mechanism of LSD1 was subsequently investigated. In the literature review, we found that LSD1 could mediate REST through demethylation.[18] Moreover, REST participates in RA progression.[19] In such context, the expression of REST was detected by RT-qPCR, which exhibited that REST was upregulated in sera and synovial tissue of RA patients (Figure 6(a) and (b)). REST was positively correlated with LSD1 in the sera of RA patients (Figure 6(c)). Although the correlation between REST and LSD1 was less obvious in
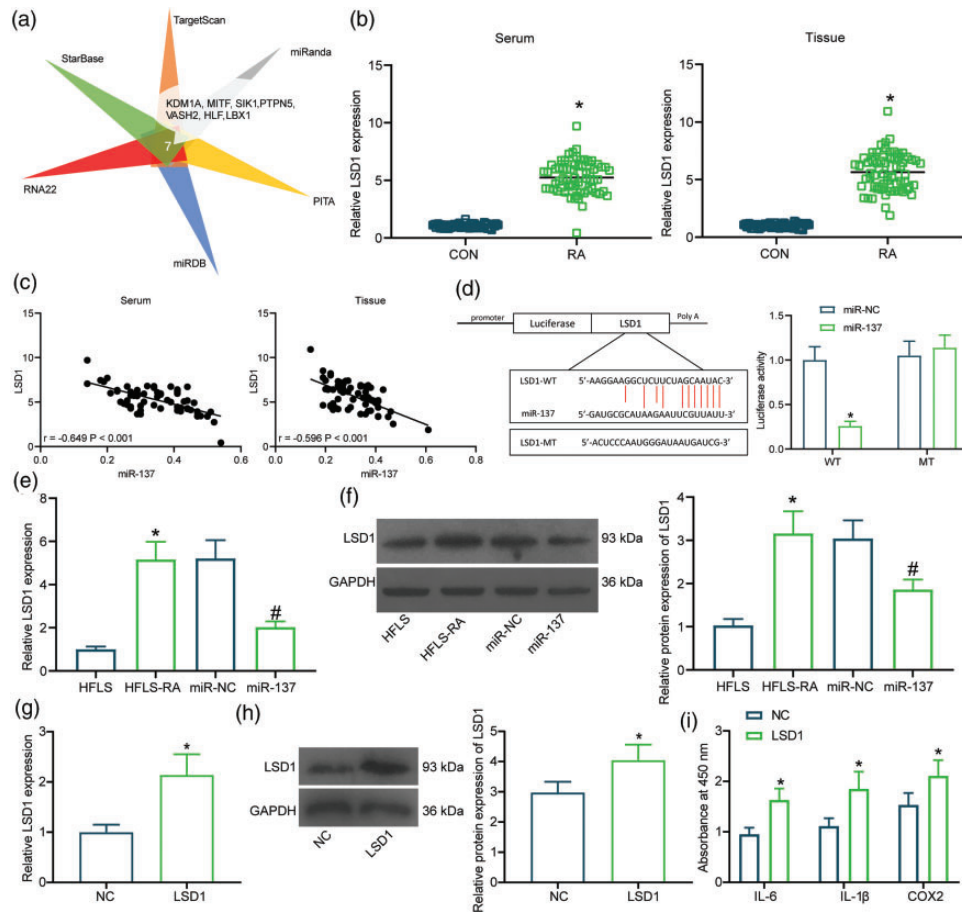
Figure 4. miR-137 targets LSD1. (a) Target genes of miR-137 predicted by bioinformatics analysis tools. (b) Expression of LSD1 in sera and synovial tissues of RA patients or healthy control determined by RT-qPCR (*p < 0.05; analyzed using two-way ANOVA). (c) Correlation analysis between LSD1 and miR-137 in sera and synovial tissues. (d) Binding relation between LSD1 and miR-137 validated by dual-luciferase reporter gene assay where WT is LSD1 wild-type plasmid, MT is LSD1 mutant plasmid (*p < 0.05; analyzed using two-way ANOVA). (e and f) Expression of LSD1 in HFLS-RA or HFLS determined by RT-qPCR and Western blot analysis (* # p < 0.05; analyzed using one-way ANOVA; *p < 0.05 vs. HFLS; # p < 0.05 miR-NC). (g and h) Expression of LSD1 in cells overexpressing LSD1 assessed by RT-qPCR and Western blot analysis (*p < 0.05; analyzed using unpaired t-test). (i) Levels of pro-inflammatory factors in cells overexpressing LSD1 detected by ELISA (*p < 0.05; analyzed using two-way ANOVA). All samples were prepared in triplicate and all measures were performed three times. miR, microRNA; LSD1, lysine-specific demethylase-1; RA, rheumatoid arthritis; ANOVA, analysis of variance; IL, interleukin; COX2, cyclooxygenase-2; HFLS, human fibroblast-like synoviocytes; ELISA, enzyme-linked immunosorbent assay.

synovial tissues than that in serum, the positive correlation was still confirmed (Figure 6(d)). Quantitative analysis of REST in cells showed that REST expression in HFLS-RA was much higher than that in HFLS, and overexpression of LSD1 resulted in upregulation of REST (Figure 6(e)). Furthermore, we upregulated the expression of REST in cells alone or in combination with miR-137 mimic or LSD1 (Figure 6(f)). As expected, REST not only remarkably elevated levels of pro-inflammatory factors, but also reversed the anti-inflammatory effects of miR-137 and accentuated the pro-inflammatory effects of LSD1 on HFLS-RA (Figure 6(g)). It was also found that LSD1 was enriched in REST in HFLS-RA by ChIP assay (Figure 6(h)).

These findings suggested that REST might be a downstream effector of LSD1 in RA.

REST mediates the mTOR pathway in RA

The activity of the mTOR pathway was further found to be distinctly increased in cells overexpressing REST, which was reversed by a mTOR inhibitor (Figure 7(a) and (b)). Moreover, ELISA results showed that when mTOR activity was dampened, the levels of inflammatory factors were remarkably lowered (Figure 7(c)). Meanwhile, miR-137 overexpression resulted in a significant downregulation of the mTOR pathway activity, and REST reversed the effects of miR-137 to increase
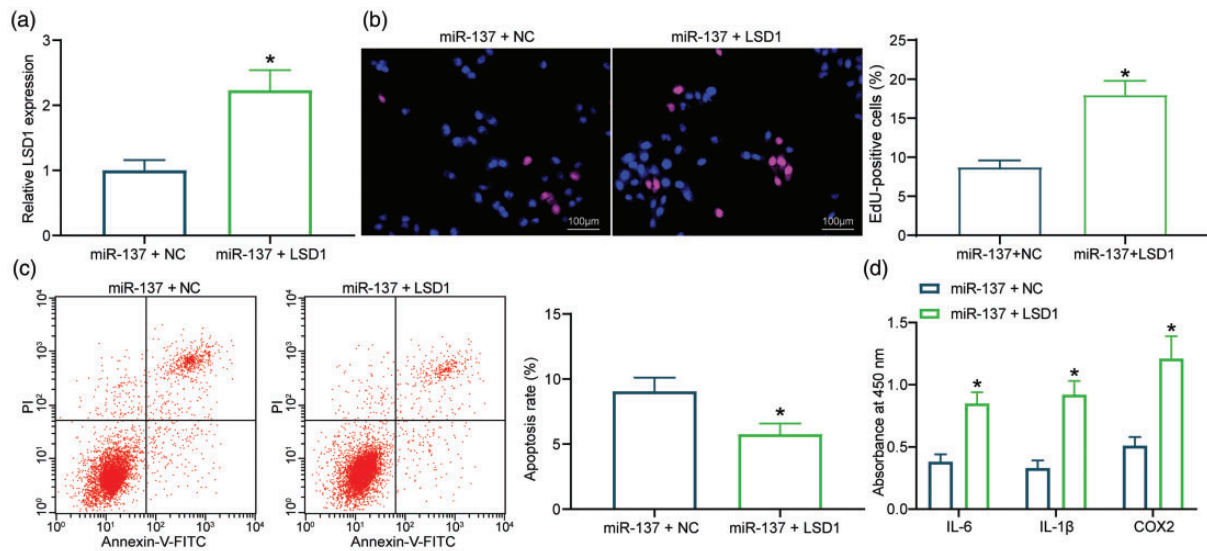
Figure 5. LSD1 reverses the inhibiting effects of miR-137 on HFLS-RA viability. (a) LSD1 expression in cells overexpressing both miR-137 and LSD1 detected by RT-qPCR (*$p < 0.05$; analyzed using unpaired *t*-test). (b) Viability of cells overexpressing both miR-137 and LSD1 detected by EdU assay (*$p < 0.05$; analyzed using unpaired *t*-test). (c) Apoptosis of cells overexpressing both miR-137 and LSD1 detected by flow cytometry (*$p < 0.05$; analyzed using unpaired *t*-test). (d) Levels of pro-inflammatory factors analyzed by ELISA (*$p < 0.05$; analyzed using two-way ANOVA). All samples were prepared in triplicate and all measures were performed three times. miR, microRNA; LSD1, lysine-specific demethylase-1; RA, rheumatoid arthritis; ANOVA, analysis of variance; HFLS, human fibroblast-like synoviocytes; ELISA, enzyme-linked immunosorbent assay; EdU, 5-Ethynyl-2'-deoxyuridine.

the mTOR pathway activity again (Figure 7(d)). Our results indicated that mTOR was mediated by REST in RA.

Overexpression of miR-137 downregulates LSD1 and impairs the REST/mTOR pathway to alleviate RA in vivo

We further validated our aforesaid results *in vivo*. After successful establishment of RA rat model, swelling and redness were observed in the hind paw of RA rats, with increased arthritic scores (Figure 8(a)). Meanwhile, the rats in the control group had normal diets and good health, while the rats in the RA group lost weight, ate less, had yellowish fur and limp feet, consistent with the range of mild to moderate pain manifestations (Figure 8(b)). Moreover, synovial tissue hyperplasia and inflammatory cell infiltration were observed under the microscope (Figure 8(c)). Next, miR-137, LSD1, or REST were overexpressed while mTOR was impaired using mTOR inhibitor-3 *in vivo*, alone or in combination, followed by arthritic scoring and pain scoring. It was observed that overexpression of miR-137 significantly reduced pain scores in rats, and LSD1 inhibited the effect of miR-137 to increase pain scores. Moreover, REST aggravated pain again in rats, and inhibition of the mTOR pathway inhibited the effect of REST to significantly reduce pain in rats (Figure 8(d)). Furthermore, overexpression of miR-137 treatment led to the lowest

score *in vivo*, along with the pronounced alleviating role in swelling and redness. However, overexpressed LSD1 reversed the effects of miR-137 on rats, which aggravated the degree of arthritis in rats. The simultaneous overexpression of REST and LSD1 worsened arthritis in rats relative to the treatment of overexpression LSD1 alone, while mTOR pathway blockage reversed the impacts of REST overexpression on rats, leading to abated arthritis *in vivo* (Figure 8(e)). Furthermore, HE staining unraveled that overexpression of miR-137 reduced inflammatory cell infiltration, while LSD1 and REST overexpression caused the most severe synovial hyperplasia and inflammatory cell infiltration *in vivo* (Figure 8(f)). Detection of gene expression in rat synovial tissues revealed that miR-137 was downregulated, and REST and LSD1 were upregulated in RA tissues. In addition, gene overexpression plasmids were stably expressed in rat synovial tissues (Figure 8(g)).

Discussion

A number of investigations have shown that miRNAs exert great effects on several autoimmune diseases, including RA.[24] Besides, miRNAs could regulate joint inflammation in RA, which suggests that miRNAs may have potential to function as novel biomarkers for therapeutic response in RA.[25] Thus, a better understanding of miRNA-based mechanism may not only illuminate the pathogenesis of RA, but also shed light on potential
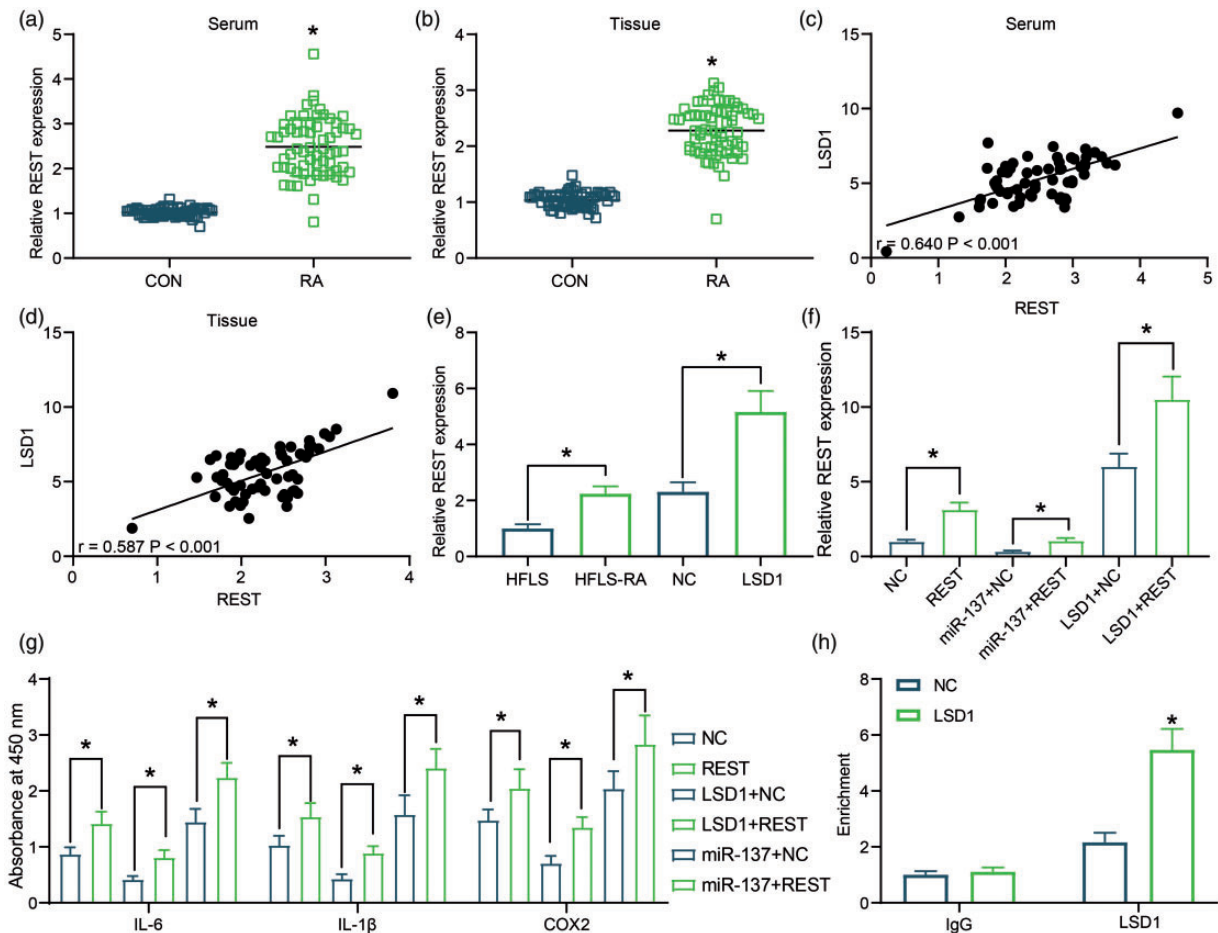
Figure 6. REST is the downstream gene of LSD1. (a and b) REST expression in sera and synovial tissues of RA patients and healthy control determined by RT-qPCR (*$p < 0.05$; analyzed using unpaired t-test). (c and d) Correlation of LSD1 and REST in serum and synovial tissues. (e) REST expression in cells overexpressing LSD1 examined by RT-qPCR (*$p < 0.05$; analyzed using one-way ANOVA). (f) REST expression in cells overexpressing REST examined by RT-qPCR (*$p < 0.05$; analyzed using one-way ANOVA). (g) Levels of pro-inflammatory factors examined using ELISA (*$p < 0.05$; analyzed using two-way ANOVA). (h) Enrichment of LSD1 in REST detected by ChIP assay (*$p < 0.05$; analyzed using two-way ANOVA). All samples were prepared in triplicate and all measures were performed three times. REST, repressor element-1 silencing transcription factor; LSD1, lysine-specific demethylase-1; RT-qPCR, reverse transcription quantitative polymerase chain reaction; RA, rheumatoid arthritis; ANOVA, analysis of variance; HFLS, human fibroblast-like synoviocytes; ELISA, enzyme-linked immunosorbent assay; ChIP, chromatin immunoprecipitation.

approaches for controlling or even preventing RA. Our study aimed to reveal the therapeutic role of miR-137 in RA.

One fundamental finding of our study highlighted that miR-137 was a potential therapeutic biomarker for RA, which was downregulated in the sera and synovial tissues of RA patients. Consistently, a previous study also reported that miR-137 expression was decreased in HFLS-RA, and overexpressed miR-137 reduced growth, migration and invasion, which decreased the inflammatory cytokine levels in RA[10]. Our results also showed that highly expressed miR-137 weakened HFLS-RA growth and arrested more cells at the G0/G1 phase, but less cells at the S phase. Increased proportion of apoptotic cells is manifested by more cells

arrested in the G0/G1 phase but less cells in the S phase.[26] Therefore, our results proved that overexpression of miR-137 accelerated apoptosis of HFLS-RA. Moreover, our ELISA results found that proinflammatory factors, involving IL-1β, IL-6 and COX2, were downregulated by overexpression of miR-137. Inflamed HFLS is one of the factors contributing to development of RA.[27] As published literature shown, IL-1β, IL-6 and COX2 are typical proinflammatory genes.[28] Therefore, our results suggested that ectopic expression of miR-137 abated inflammatory response in HFLS-RA, which displayed that miR-137 exerted an inhibiting role in RA development.

Another important finding was derived from our mechanistic investigation, which showed that miR-137
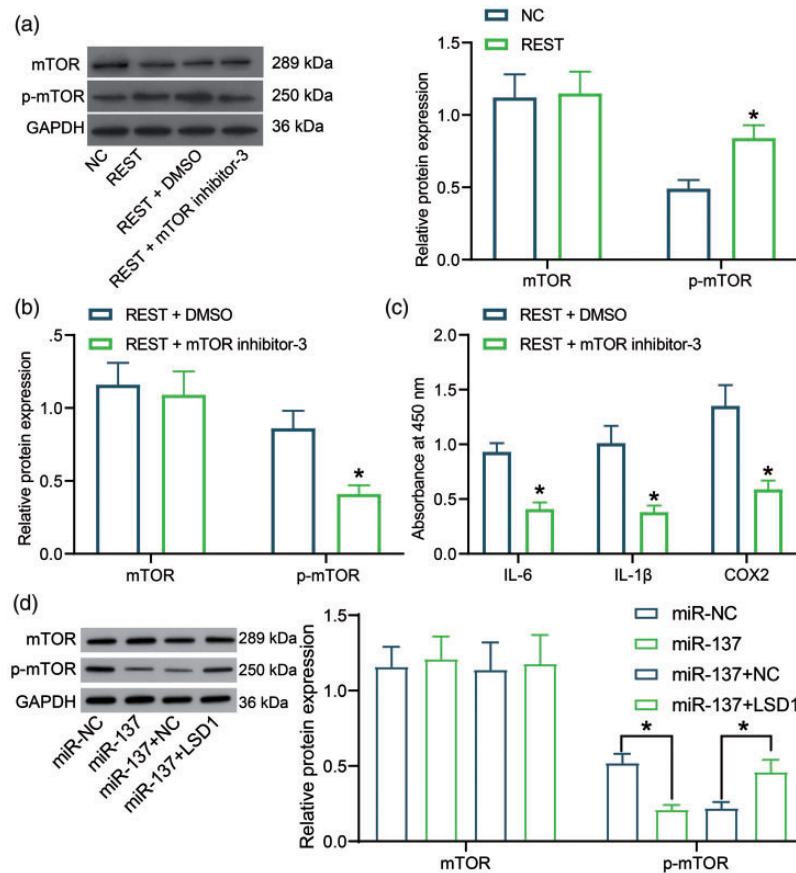
Figure 7. mTOR pathway is regulated by REST in RA. (a and b) Expression of mTOR and extent of mTOR phosphorylation in the cells examined using Western blot analysis (*$p < 0.05$; analyzed using two-way ANOVA). (c) Levels of pro-inflammatory factors in cells over-expressing REST treated with mTOR inhibitor and determined by ELISA (*$p < 0.05$; analyzed using two-way ANOVA). (d) Expression of mTOR and extent of mTOR phosphorylation in the cells examined using Western blot analysis (*$p < 0.05$; analyzed using two-way ANOVA). All samples were prepared in triplicate and all measures were performed three times. REST, repressor element-1 silencing transcription factor; mTOR, mammalian target of rapamycin; ANOVA, analysis of variance; ELISA, enzyme-linked immunosorbent assay.

targeted LSD1 to suppress LSD1 expression. As our results exhibited, LSD1 was upregulated in the sera and synovial tissues of RA patients. LSD1 expression has also been illustrated to be reduced in RA, and knockdown of LSD1 by plasmid transfection could ameliorate severity of RA *in vitro* and *in vivo*,[16] which is similar to our results. Additionally, LSD1 is a downstream gene of miR-137-3p, which could be negatively regulated by miR-137-3p in dorsal root ganglion neurons.[29] miR-137 was able to suppress oncogene LSD1 in non-small cell lung cancer by inhibiting the cell proliferation.[30] What has been discussed above supports our result that miR-137 targeted LSD1. Moreover, the interaction between LSD1 and REST has been underscored in neuroblastoma and medulloblastoma cells.[31,32] Furthermore, we found that REST/mTOR pathway was linked to the downstream mechanism of LSD1. The evidence collected from our study showed that REST expression was positively correlated with the level of LSD1, while mTOR pathway activity was

more active as REST expression increased. Although the study on the role of REST/mTOR pathway in RA is limited, impacts of REST or mTOR alone on RA has been elaborated previously. For instance, REST, being negatively correlated with miR-9-5p expression, promoted inflammatory damage in RA.[19] Also, impaired mTOR pathway by protocatechuic acid contributed to RA alleviation.[33] Based on these literatures, it was reasonable to infer that miR-137 attenuated RA by suppressing the expression of its target gene LSD1, which inhibited the activation of the REST/mTOR pathway.

Finally, to validate our results *in vivo,* we applied CIA to induce RA rat model. CIA has been widely used in RA animal model establishment, which is often linked to joint dysfunction and damage of articular cartilage.[34] Our study showed that overexpressed miR-137 or suppressed mTOR pathway could reduce the degree of swelling, as well as lessened synovial hyperplasia and inflammatory cell infiltration. Previous literature shows that reduced arthritic scores are correlated with less
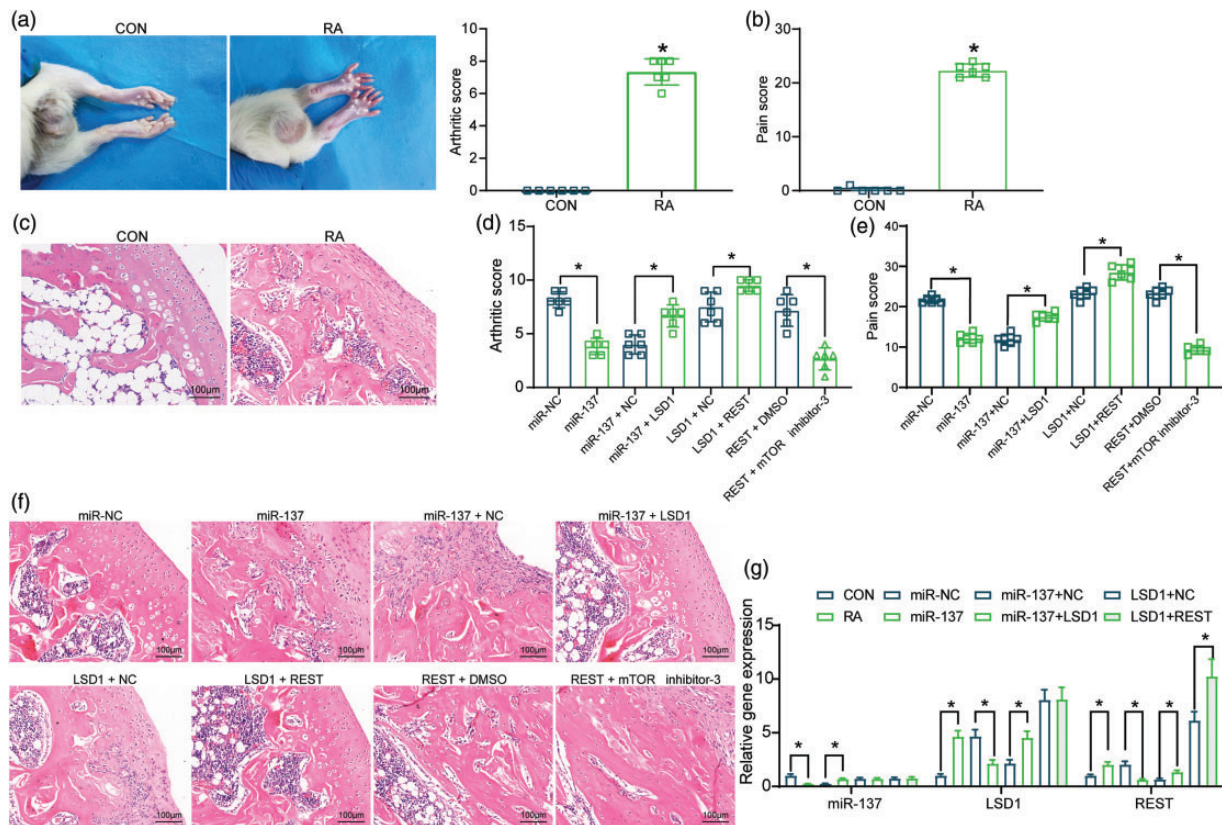
Figure 8. miR-137/LSD1/REST/mTOR axis mediates RA *in vivo*. (a) Arthritic scoring of RA rats induced by CIA (*$p < 0.05$; analyzed using unpaired *t*-test). (b) Pain scores of RA rats induced by CIA (*$p < 0.05$; analyzed using unpaired *t*-test). (c) Synovial tissue hyperplasia and inflammatory cell infiltration observed using HE staining. (d) Pathological change of arthritis after gain- and loss-of-function experiments (*$p < 0.05$; analyzed using one-way ANOVA). (e) Pain scores of RA rats induced by CIA after gain- and loss-of-function experiments (*$p < 0.05$; analyzed using one-way ANOVA). (f) Synovial tissues of differently treated rats observed using HE staining. (g) Detection of gene expression in tissues by RT-qPCR (*$p < 0.05$; analyzed using two-way ANOVA). miR, microRNA; LSD1, lysine-specific demethylase-1; REST, repressor element-1 silencing transcription factor; mTOR, mammalian target of rapamycin; CIA, collagen type II-induced arthritis; ANOVA, analysis of variance; HE, hematoxylin-eosin.
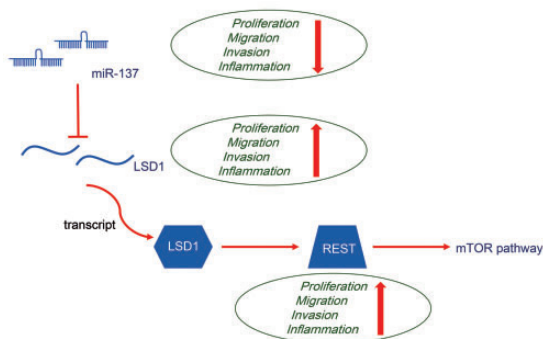

Figure 9. Schematic diagram showing that miR-137-targeted downregulation of LSD1 could suppress the REST/mTOR pathway, which hinders the progression of RA. miR, microRNA; LSD1, lysine-specific demethylase-1; REST, repressor element-1 silencing transcription factor; mTOR, mammalian target of rapamycin; RA, rheumatoid arthritis.

swelling, reductions in synovial inflammatory cell infiltration and synovial hyperplasia.[35] Therefore, we believed that the results *in vitro* were reproduced *in vivo*.

In conclusion, our findings demonstrate that miR-137 is a potential therapeutic target for RA, which could suppress growth, migration/invasion, and inflammatory response among HFLS-RA, and alleviate RA by reducing infiltration of inflammatory cells *in vivo,* which was achieved by inhibition of LSD1 expression and blockage of the REST/mTOR pathway (Figure 9). Our results have illustrated a framework for the miRNA-based strategy to the development of new therapeutics for RA. Consequently, the mechanism of miR-137/LSD1/REST/mTOR pathway highlighted as a promising therapeutic target for RA patients. However, more studies are needed to translate the miRNA-based treatment from animal studies to human use.

Declaration of conflicting interests

Funding

ORCID iD

Guanghui Wang https://orcid.org/0000-0002-6165-0811

References

1. Miao C-g, Yang Y-y, He X, Li X-f, Huang C, Huang Y, Zhang L, Lv X-W, Jin Y, Li J. Wnt signaling pathway in rheumatoid arthritis, with special emphasis on the different roles in synovial inflammation and bone remodeling. *Cell Signal* 2013; 25: 2069–2078.

2. Wegner N, Lundberg K, Kinloch A, Fisher B, Malmström V, Feldmann M, Venables PJ. Autoimmunity to specific citrullinated proteins gives the first clues to the etiology of rheumatoid arthritis. *Immunol Rev* 2010; 233: 34–54.

3. Muller-Ladner U, Ospelt C, Gay S, Distler O, Pap T. Cells of the synovium in rheumatoid arthritis. Synovial fibroblasts. *Arthritis Res Ther* 2007; 9: 223.

4. Nygaard G, Firestein GS. Restoring synovial homeostasis in rheumatoid arthritis by targeting fibroblast-like synoviocytes. *Nat Rev Rheumatol* 2020; 16: 316–333.

5. Pap T, Dankbar B, Wehmeyer C, Korb-Pap A, Sherwood J. Synovial fibroblasts and articular tissue remodelling: role and mechanisms. *Semin Cell Dev Biol* 2020; 101: 140–145.

6. Long L, Yu P, Liu Y, Wang S, Li R, Shi J, Zhang X, Li Y, Sun X, Zhou B, Cui L, Li Z. Upregulated microRNA-155 expression in peripheral blood mononuclear cells and fibroblast-like synoviocytes in rheumatoid arthritis. *Clin Dev Immunol* 2013; 2013: 296139.

7. Shi DL, Shi GR, Xie J, Du XZ, Yang H. MicroRNA-27a inhibits cell migration and invasion of Fibroblast-Like synoviocytes by targeting Follistatin-Like protein 1 in rheumatoid arthritis. *Mol Cells* 2016; 39: 611–618.

8. Xu T, Huang C, Chen Z, Li J. MicroRNA-323-3p: a new biomarker and potential therapeutic target for rheumatoid arthritis. *Rheumatol Int* 2014; 34: 721–722.

9. Liu Q, Chen YQ. A new mechanism in plant engineering: the potential roles of microRNAs in molecular breeding for crop improvement. *Biotechnol Adv* 2010; 28: 301–307.

10. Du J, Zhang F, Guo J. miR137 decreases proliferation, migration and invasion in rheumatoid arthritis fibroblast-like synoviocytes. *Mol Med Rep* 2018; 17: 3312–3317.

11. Wang J, Fang L, Ye L, et al. miR-137 targets the inhibition of TCF4 to reverse the progression of osteoarthritis through the AMPK/NF-kappaB signaling pathway. *Biosci Rep* 2020; 40: BSR20200466.

12. Zhang Y, Wang G, Ma L, Wang C, Wang L, Guo Y, Zhao X. miR-137 suppresses cell growth and extracellular matrixdegradation through regulating ADAMTS-5 in chondrocytes. *Am J Transl Res* 2019; 11: 7027–7034.

13. Kyzar EJ, Bohnsack JP, Zhang H, Pandey SC. MicroRNA-137 drives epigenetic reprogramming in the adult amygdala and behavioral changes after. *Adolescent Alcohol Exposure. eNeuro* 2019; 6

14. Gu F, Lin Y, Wang Z, Wu X, Ye Z, Wang Y, Lan H. Biological roles of LSD1 beyond its demethylase activity. *Cell Mol Life Sci* 2020; 77: 3341–3350.

15. Niwa H, Sato S, Handa N, Sengoku T, Umehara T, Yokoyama S. Development and structural evaluation of N-Alkylated trans-2-Phenylcyclopropylamine-Based LSD1 inhibitors. *ChemMedChem* 2020; 15: 787–793.

16. Liu W, Fan J-B, Xu D-W, Zhu X-H, Yi H, Cui S-Y, Zhang J, Cui Z-M. Knockdown of LSD1 ameliorates the severity of rheumatoid arthritis and decreases the function of CD4 T cells in mouse models. *Int J Clin Exp Pathol* 2018; 11: 333–341.

17. Sun J, Feng H, Xing W, et al. Histone demethylase LSD1 is critical for endochondral ossification during bone fracture healing. *Sci Adv* 2020; 6: eaaz1410.

18. Jin Y, Ma D, Gramyk T, Guo C, Fang R, Ji H, Shi YG. Kdm1a promotes SCLC progression by transcriptionally silencing the tumor suppressor rest. *Biochem Biophys Res Commun* 2019; 515: 214–221.

19. Li Z, Li Y, Li Q, Zhang Z, Jiang L, Li X. Role of miR-9-5p in preventing peripheral neuropathy in patients with rheumatoid arthritis by targeting REST/miR-132 pathway. *In Vitro Cell Dev Biol Anim* 2019; 55: 52–61.

20. Du H, Zhang X, Zeng Y, Huang X, Chen H, Wang S, Wu J, Li Q, Zhu W, Li H, Liu T, Yu Q, Wu Y, Jie L. A novel phytochemical, DIM, inhibits proliferation, migration, invasion and TNF-alpha induced inflammatory cytokine production of synovial fibroblasts from rheumatoid arthritis patients by targeting MAPK and AKT/mTOR signal pathway. *Front Immunol* 2019; 10: 1620.

21. Wang J, Zhao Q. Kaempferitrin inhibits proliferation, induces apoptosis, and ameliorates inflammation in human rheumatoid arthritis fibroblast-like synoviocytes. *Phytother Res* 2019; 33: 1726–1735.

22. Tao Y, Wang Z, Wang L, Shi J, Guo X, Zhou W, Wu X, Liu Y, Zhang W, Yang H, Shi Q, Xu Y, Geng D. Downregulation of miR-106b attenuates inflammatory responses and joint damage in collagen-induced arthritis. *Rheumatology (Oxford)* 2017; 56: 1804–1813.

23. Dai Q, Zhou D, Xu L, Song X. Curcumin alleviates rheumatoid arthritis-induced inflammation and synovial hyperplasia by targeting mTOR pathway in rats. *Drug Des Devel Ther* 2018; 12: 4095–4105.

24. Zhang L, Wu H, Zhao M, Chang C, Lu Q. Clinical significance of miRNAs in autoimmunity. *J Autoimmun* 2020; 109: 102438.

25. Furer V, Greenberg JD, Attur M, Abramson SB, Pillinger MH. The role of microRNA in rheumatoid arthritis and other autoimmune diseases. *Clin Immunol* 2010; 136: 1–15.

26. Zhang X, Feng H, Du J, Sun J, Li D, Hasegawa T, Amizuka N, Li M. Aspirin promotes apoptosis and inhibits proliferation by blocking G0/G1 into S phase in rheumatoid arthritis fibroblast-like synoviocytes via downregulation of JAK/STAT3 and NF-kappaB signaling pathway. *Int J Mol Med* 2018; 42: 3135–3148.

27. Lahoti TS, John K, Hughes JM, Kusnadi A, Murray IA, Krishnegowda G, Amin S, Perdew GH. Aryl hydrocarbon receptor antagonism mitigates cytokine-mediated inflammatory signalling in primary human fibroblast-like synoviocytes. *Ann Rheum Dis* 2013; 72: 1708–1716.

28. Morand EF, Leech M. Macrophage migration inhibitory factor in rheumatoid arthritis. *Front Biosci* 2005; 10: 12–22.

29. Chen L, Wang X, Huang W, Ying T, Chen M, Cao J, Wang M. MicroRNA-137 and its downstream target LSD1 inversely regulate anesthetics-induced neurotoxicity in dorsal root ganglion neurons. *Brain Res Bull* 2017; 135: 1–7.

30. Zhang X, Zhang X, Yu B, Hu R, Hao L. Oncogene LSD1 is epigenetically suppressed by miR-137 overexpression in human non-small cell lung cancer. *Biochimie* 2017; 137: 12–19.

31. Callegari K, Maegawa S, Bravo-Alegria J, Gopalakrishnan V. Pharmacological inhibition of LSD1 activity blocks REST-dependent medulloblastoma cell migration. *Cell Commun Signal* 2018; 16: 60.

32. Chen K, Cai Y, Cheng C, Zhang J, Lv F, Xu G, Duan P, Wu Y, Wu Z. MYT1 attenuates neuroblastoma cell differentiation by interacting with the LSD1/CoREST complex. *Oncogene* 2020; 39: 4212–4226.

33. Wu H, Wang J, Zhao Q, Ding Y, Zhang B, Kong L. Protocatechuic acid inhibits proliferation, migration and inflammatory response in rheumatoid arthritis fibroblast-like synoviocytes. *Artif Cells Nanomed Biotechnol* 2020; 48: 969–976.

34. Wu J, Fan KJ, Wang QS, Xu BX, Cai Q, Wang TY. DMY protects the knee joints of rats with collagen-induced arthritis by inhibition of NF-kappaB signaling and osteoclastic bone resorption. *Food Funct* 2020; 11: 6251–6264.

35. Wang M, Li H, Wang Y, Hao Y, Huang Y, Wang X, Lu Y, Du Y, Fu F, Xin W, Zhang L. Anti-Rheumatic properties of gentiopicroside are associated with suppression of ROS-NF-kappaB-NLRP3 axis in Fibroblast-Like synoviocytes and NF-kappaB pathway in Adjuvant-Induced arthritis. *Front Pharmacol* 2020; 11: 515.